Mechanics of Advanced Composite Structures 5 (2018) 187 - 198

Semnan University

Mechanics of Advanced Composite Structures

journal homepage: http://MACS.journals.semnan.ac.ir

# Thermoelastic Interaction in a Three-Dimensional Layered Sandwich Structure

**A. Sur*, M. Kanoria**

*Department of Applied Mathematics, University of Calcutta, 92 A. P. C. Road, Kolkata 700009, India*

**PAPER INFO**

***Paper history:***
Received 2018-03-05
Received in revised form 2018-06-13
Accepted 2018-06-15

***Keywords:***
Generalized thermoelasticity
Dual-phase-lag thermoelastic-model
Hyperbolic heat conduction
Finite wave speed
Normal mode analysis

**ABSTRACT**

The present article investigates the thermoelastic interaction in a three-dimensional homogeneous and isotropic sandwich structure using the dual-phase-lag (DPL) model of generalized thermoelasticity. The incorporated resulting non-dimensional coupled equations are applied to a specific problem in which a sandwich layer of unidentical homogeneous and isotropic substances is subjected to time-dependent thermal loadings; the two outer sides are traction-free. The analytical expressions for the displacement components, stress, temperature, and strain are obtained in the physical domain using the normal mode analysis. The mathematical difficulties in dealing with the hyperbolic heat conduction equation are overcome and the thermophysical quantities of the sandwich structure are depicted graphically. The effect that the two phase lags have on the studied field are highlighted. The results demonstrate the phenomenon of a finite speed of wave propagation in a sandwich structure for each field.



## 1. Introduction

The conventional dynamic theory of thermoelasticity is based on the hypothesis of Fourier's law of heat conduction in which the temperature distribution is governed by a parabolic-type partial differential equation. Thus, the theory predicts that a thermal signal is felt instantaneously everywhere in a body. This implies that there is an infinite speed of propagation of the thermal signal, which is unrealistic from a physical point of view, especially for short-time responses. It is also well known that heat transmission at low temperatures propagates by means of waves. These aspects have aroused much interest and activity in the field of heat propagation and given rise to the subject of generalized thermoelasticity. Generalized thermoelasticity theories involve hyperbolic-type governing equations and the finite speed of thermal signals. Lord and Shulman [1] proposed an extended thermoelasticity theory that involves one thermal relaxation time. Green and Lindsay [2] proposed a temperature-rate-dependent theory of thermoelasticity that includes two relaxation times. These generalized models are familiar to many researchers and numerous studies have been done using these theories.

Green and Naghdi [3-5] introduced three models, which are subsequently referred to as models I, II, and III, to provide sufficient basic modifications in the constitutive equations in order to permit the treatment of a wide class of heat flow problems. The Green and Naghdi models include a term called the thermal displacement gradient among the independent constitutive variables. Although the thermal wave model can capture the microscale response in time, it does not capture the microscale response in space [6]. Therefore, the validity of the thermal wave model becomes debatable for the fast transient responses with respect to microstructural interactions [7]. To remove the precedence assumption implied

*Corresponding author. Tel.: +91-9830648301.
*E-mail address: abhiksur4@gmail.com*
DOI: 10.22075/MACS.2018.13517.1134

by the thermal wave model, the dual-phase-lag (DPL) model of heat conduction was developed [8] and verified [7]. The model accounts for the spatial and temporal effects of both macroscale and microscale heat transfer for one temperature formulation with the form: $\vec{q}(P,t+\tau_q) = -K\vec{\nabla}T(P,t+\tau_T)$, where $\tau_T$ is the phase lag of the temperature gradient. In the DPL model with $\tau_q > \tau_T$, the temperature gradient within the medium induces heat flux; hence, the temperature gradient is the cause of the energy transport and the heat flux is the effect. However, for $\tau_q < \tau_T$, the heat flux is the cause of the energy transport and the temperature gradient is the effect. For $\tau_q = \tau_T$ with a homogeneous initial temperature, the DPL model reduces to Fourier's law [9].

Prasad, Kumar, and Mukhopadhyay [10] studied the propagation of finite thermal waves in the context of the DPL model. El-Karamany and Ezzat [11] recently solved some remarkable problems using the DPL model. Chiriţă [12] studied the time-differential DPL model. Sur, Pal and Kanoria [13–16] produced several remarkable works on finite thermal wave propagations in generalized thermoelasticity.

Modern structural elements are often subjected to temperature changes of such magnitude that their material properties are considered to no longer have constant values [17]. Because the thermal and mechanical properties of materials vary with temperature, it must be taken into consideration during the thermal stress analysis of these materials [18-22].

One of the major subjects of the mechanics of multilayered composites is the elaboration of the mathematical modeling, methods, and algorithms used for the numerical solutions of engineering problems. One class of interesting elastodynamic problems has a wide range of applications not only in the mechanics of composite materials, but also in other branches of modern engineering. Therefore, a large number of theoretical and computational investigations have been reported in this field, and a systematic review of the obtained results is available in a series of monographs [23–25].

It is widely accepted that an inappropriate selection of interface elements can lead to regions of unrealistically high stress gradients and erroneous results. Considering the fact that many media are naturally layered, some researchers have shifted their focus to the study of thermoelastic problems in a multilayered medium. Vishwakarma [26] reported on the torsional wave propagation in a reinforced sandwich medium. Tokovyy and Ma [27] presented an analytical solution for the axisymmetric and transient-thermoelastic problem of body forces and a heat source in vertically inhomogeneous media. Wu [28] proposed an analytical theory of the nonlinear unstable pavement temperature fields for a 2D layered composite structure; the theory was based on the fundamental principles of meteorology thermodynamics. The exact solution of the transient analysis of a multilayered magneto-electro-thermoelastic strip subjected to a nonuniform heat supply has also been reported [29]. Zhong and Geng [30] demonstrated the solutions of thermal stress problems of a multilayered elastic half-space using the transfer matrix method. Sur and Kanoria [31] studied the problem of generalized thermoelasticity for different composite structures.

The objective of this paper is to consider three-dimensional thermoelastic layers of unidentical substances, each of which is homogeneous and isotropic. The outer surfaces of the medium are free of tractions and are subjected to time-dependent thermal loadings. The heat conduction equation has been formulated to incorporate the DPL model of heat conduction. Using the normal mode analysis, the governing equations have been expressed in Cartesian coordinates and are applied to a thermal shock problem in a composite structure that fills the half-space. The numerical estimates of the thermophysical quantities have been computed for copper and stainless steel, and are depicted graphically. To the best of the authors' knowledge, this is the first time that a problem based on DPL heat conduction has been modeled. Excellent predictive capability is demonstrated in the layered composite structure due to the DPL heat conduction model.

## 2. Basic Equations

The stress-strain-temperature relations are as follows:

$$\sigma_{ij} = 2\mu e_{ij} + [\lambda\Delta - \gamma\theta]\delta_{ij}, \quad i, j = 1,2,3 \tag{1}$$

where $\sigma_{ij}$ is the stress tensor, $\theta$ is the temperature field, $\Delta$ the cubical dilation, $\lambda$ and $\mu$ are Lamé's constants, $\gamma = (3\lambda + 2\mu)\alpha_t$, $\alpha_t$ is the coefficient of linear thermal expansion, and $\delta_{ij}$ is the Kronecker delta. In addition, $\Delta = e_{ii}$ and $e_{ij}$ is the strain tensor given by:

$$e_{ij} = \frac{1}{2}\left(u_{i,j} + u_{j,i}\right). \tag{2}$$

The stress equation of motion in the absence of body force is

$$\sigma_{ij,j} = \rho\ddot{u}_i, \quad i, j = 1,2,3 \tag{3}$$

The heat equation for the dynamic coupled generalized thermoelasticity based on the DPL thermoelasticity model is given by:

$$K\left(1+\tau_T\frac{\partial}{\partial t}\right)\nabla^2\theta = \left(1+\tau_q\frac{\partial}{\partial t}+\frac{\tau_q^2}{2}\frac{\partial^2}{\partial t^2}\right)\left(\rho c_v\dot{\theta}+\gamma\theta_0\dot{e}\right). \tag{4}$$

where $u_i$ $(i=1,2,3)$ is the displacement components, $\rho$ is the density, and $c_v$ is the specific heat at constant strain.

## 3. Formulation of the Problem

We now consider an isotropic, homogeneous, and thermoelastic layered medium of a sandwich structure with a three-dimensional space that fills the region $\Omega$, which is defined as $\Omega=\{(x,y,z):-2l\le x\le 2l,-\infty<y<\infty,-\infty<z<\infty\}$ where layers I and III are made from same material and layer II is a different material. Layer II is in the middle of the space and its thickness is half of the entire thickness. We consider that the outer sides of the medium are thermally shocked and traction-free. The rectangular Cartesian system $(x,y,z)$ is used in which the origin is on the surface $x=0$. The components of the displacement vector $\vec{u}$ are given as $(u,v,w)$.

The constitutive relations are as follows:

$$\sigma_{xx}=2\mu\frac{\partial u}{\partial x}+\lambda e-\gamma\theta, \tag{5}$$

$$\sigma_{yy}=2\mu\frac{\partial v}{\partial y}+\lambda e-\gamma\theta, \tag{6}$$

$$\sigma_{zz}=2\mu\frac{\partial w}{\partial z}+\lambda e-\gamma\theta, \tag{7}$$

$$\sigma_{xy}=\mu\left(\frac{\partial u}{\partial y}+\frac{\partial v}{\partial x}\right), \tag{8}$$

$$\sigma_{yz}=\mu\left(\frac{\partial v}{\partial z}+\frac{\partial w}{\partial y}\right), \tag{9}$$

$$\sigma_{zx}=\mu\left(\frac{\partial u}{\partial z}+\frac{\partial w}{\partial x}\right), \tag{10}$$

The equations of motion in the absence of body forces are

$$(\lambda+2\mu)\frac{\partial^2 u}{\partial x^2}+\mu\left(\frac{\partial^2 u}{\partial y^2}+\frac{\partial^2 u}{\partial z^2}\right)+(\lambda+\mu)\left(\frac{\partial^2 v}{\partial x\partial y}+\frac{\partial^2 w}{\partial x\partial z}\right)-\gamma\frac{\partial\theta}{\partial x}=\rho\ddot{u}, \tag{11}$$

$$(\lambda+2\mu)\frac{\partial^2 v}{\partial y^2}+\mu\left(\frac{\partial^2 v}{\partial x^2}+\frac{\partial^2 v}{\partial z^2}\right)+(\lambda+\mu)\left(\frac{\partial^2 u}{\partial x\partial y}+\frac{\partial^2 w}{\partial y\partial z}\right)-\gamma\frac{\partial\theta}{\partial y}=\rho\ddot{v}, \tag{12}$$

$$(\lambda+2\mu)\frac{\partial^2 w}{\partial z^2}+\mu\left(\frac{\partial^2 w}{\partial x^2}+\frac{\partial^2 w}{\partial y^2}\right)+(\lambda+\mu)\left(\frac{\partial^2 u}{\partial x\partial z}+\frac{\partial^2 v}{\partial y\partial z}\right)-\gamma\frac{\partial\theta}{\partial z}=\rho\ddot{w}, \tag{13}$$

The heat conduction equation for the DPL model is given by:

$$K\left(1+\tau_T\frac{\partial}{\partial t}\right)\left(\frac{\partial^2\theta}{\partial x^2}+\frac{\partial^2\theta}{\partial y^2}+\frac{\partial^2\theta}{\partial z^2}\right)=\left(1+\tau_q\frac{\partial}{\partial t}+\frac{\tau_q^2}{2}\frac{\partial^2}{\partial t^2}\right)\left[\rho c_v\dot{\theta}+\gamma\theta_0\frac{\partial}{\partial t}\left(\frac{\partial u}{\partial x}+\frac{\partial v}{\partial y}+\frac{\partial w}{\partial z}\right)\right], \tag{14}$$

where $\tau_T=0$. Neglecting the term $\frac{\tau_q^2}{2}$, we have the Lord–Shulman (LS) heat conduction model.

Equations (11)–(13) can be rewritten in the following form:

$$\rho\frac{\partial\ddot{u}}{\partial x}=\mu\nabla^2\frac{\partial u}{\partial x}+(\lambda+\mu)\frac{\partial^2 e}{\partial x^2}-\gamma\frac{\partial^2\theta}{\partial x^2}, \tag{15}$$

$$\rho\frac{\partial\ddot{v}}{\partial y}=\mu\nabla^2\frac{\partial v}{\partial y}+(\lambda+\mu)\frac{\partial^2 e}{\partial y^2}-\gamma\frac{\partial^2\theta}{\partial y^2}, \tag{16}$$

$$\rho\frac{\partial\ddot{w}}{\partial z}=\mu\nabla^2\frac{\partial w}{\partial z}+(\lambda+\mu)\frac{\partial^2 e}{\partial z^2}-\gamma\frac{\partial^2\theta}{\partial z^2}, \tag{17}$$

The nondimensional variables are as follows:

$$x'=c_0\eta x,\quad y'=c_0\eta y,\quad z'=c_0\eta z,$$

$$u'=c_0\eta u,\quad v'=c_0\eta v,\quad w'=c_0\eta w,\quad t'=c_0^2\eta t,$$

$$\tau_{q'}=c_0^2\eta\tau_q,\quad \tau_{T'}=c_0^2\eta\tau_T,$$

$$\theta'=\frac{\gamma_e\theta}{\rho c_0^2},\quad \sigma_{ij}{}'=\frac{\sigma_{ij}}{\rho c_0^2},$$

where

$$c_0^2 = \frac{\lambda + 2\mu}{\rho} \quad \text{and} \quad \eta = \frac{\rho c_v}{K},$$

After removing the primes, the equations can be written in a nondimensional form as follows:

$$\frac{\partial \ddot{u}}{\partial x} = \delta \nabla^2 \frac{\partial u}{\partial x} + (1-\delta)\frac{\partial^2 e}{\partial x^2} - \frac{\partial^2 \theta}{\partial x^2}, \tag{18}$$

$$\frac{\partial \ddot{v}}{\partial y} = \delta \nabla^2 \frac{\partial v}{\partial y} + (1-\delta)\frac{\partial^2 e}{\partial y^2} - \frac{\partial^2 \theta}{\partial y^2}, \tag{19}$$

$$\frac{\partial \ddot{w}}{\partial z} = \delta \nabla^2 \frac{\partial w}{\partial z} + (1-\delta)\frac{\partial^2 e}{\partial z^2} - \frac{\partial^2 \theta}{\partial z^2}, \tag{20}$$

$$\left(1 + \tau_T \frac{\partial}{\partial t}\right)\nabla^2 \theta = \left(1 + \tau_q \frac{\partial}{\partial t} + \frac{\tau_q^2}{2}\frac{\partial^2}{\partial t^2}\right)\left(\dot{\theta} + \delta_0 \dot{e}\right), \tag{21}$$

where

$$\delta_0 = \frac{\gamma^2 \theta_0}{\rho c_v (\lambda + 2\mu)} \quad \text{and} \quad \delta = \frac{\mu}{\lambda + 2\mu}$$

In a similar manner, we can transform the constitutive relations into nondimensional forms. The dimensionless expressions for the constitutive are obtained by summation of Equations (18) – (20) as follows:

$$\ddot{e} = \nabla^2 e - \nabla^2 \theta, \tag{22}$$

We shall consider the invariant stress $\sigma$ to be the mean value of the normal stresses as follows:

$$\sigma = \frac{\sigma_{xx} + \sigma_{yy} + \sigma_{zz}}{3}$$

Substituting the expressions for $\sigma_{xx}$, $\sigma_{yy}$, and $\sigma_{zz}$ into the above expressions, we obtain

$$\sigma = \delta_1 e - \theta, \text{ where } \delta_1 = \frac{3 - 4\delta}{3}. \tag{23}$$

## 4. Normal Mode Analysis

In this method, the solutions of the physical variables can be decomposed in terms of the normal modes in the following form:

$$[u, v, w, e, \theta, \sigma_{ij}](x, y, z, t) = [u^*, v^*, w^*, e^*, \theta^*, \sigma_{ij}^*](x)\, e^{[\omega t + i(my + nz)]}, \tag{24}$$

where $u^*(x)$, $v^*(x)$, $w^*(x)$, $e^*(x)$, $\theta^*(x)$ and $\sigma_{ij}^*(x)$ are the amplitudes of the functions $i = \sqrt{-1}$, $\omega$ is the angular frequency, and $m$ and $n$ are the wave numbers in the $y$ and $z$ directions, respectively.

By rewriting Equations (21) - (23) based on the normal modes and eliminating $e^*(x)$ from the resulting expressions, we obtain a system of ordinary differential equations:

$$\left(D^2 - m^2 - n^2\right)\theta^*(x) = \gamma_1 \begin{bmatrix} (\delta_0 + \delta_1)\theta^*(x) + \\ \delta_0 \sigma^*(x) \end{bmatrix}. \tag{25}$$

$$\left(D^2 - m^2 - n^2\right)\sigma^*(x) = a_1 \sigma^*(x) + a_2 \theta^*(x). \tag{26}$$

where

$$\gamma_1 = \frac{\omega\left(1 + \tau_q \omega + \frac{\tau_q^2}{2}\omega^2\right)}{\delta_1 (1 + \omega \tau_T)},$$

$$a_1 = \omega^2 - (1 - \delta_1)\delta_0 \gamma_1,$$
$$a_2 = \omega^2 - (1 - \delta_1)\gamma_1 (\delta_0 + \delta_1).$$

Eliminating $\theta^*(x)$ from Equations (25) and (26) yields the following fourth-order differential equation:

$$(D^4 - LD^2 + M)\sigma^*(x) = 0, \tag{27}$$

where

$$L = \alpha_1 + \alpha_2,$$
$$M = \alpha_1 \alpha_2 - a_2 \gamma_1 \delta_0,$$
$$\alpha_1 = m^2 + n^2 + a_1,$$
$$\alpha_2 = m^2 + n^2 + (\delta_0 + \delta_1)\gamma_1.$$

We consider the layered plates in a sandwich structure in which layers I and III are made from the same material and layer II is a different material. Layer II is placed in the middle of the plane; its thickness is equal to half thickness of the plate. We consider that the two outer sides of the sandwich structure are subjected to thermal loading and are traction-free.

(i) Region I $(-2l \le x \le -l)$ : The solutions of Equations (25) and (26) take the following form:

$$\theta^{*I} = A_1 (k_1^2 - p^2)\cosh(k_1 x) + A_2 (k_2^2 - p^2)\cosh(k_2 x), \tag{28}$$

$$\sigma^{*I} = a_2 A_1 \cosh(k_1 x) + a_2 A_2 \cosh(k_2 x), \tag{29}$$

where $p^2 = m^2 + n^2 + a_1$ and $k_1$ and $k_2$ are the roots of the equation

$$k^4 - L^I k^2 + M^I = 0, \tag{30}$$

(ii) Region II $(-l \le x \le l)$ : The solutions of Equations (25) and (26) take the following form:

$$\theta^{*II} = B_1(p_1^2 - p^2)\cosh(p_1 x) + B_2(p_2^2 - p^2)\cosh(p_2 x), \quad (31)$$

$$\sigma^{*II} = a_2 B_1 \cosh(p_1 x) + a_2 B_2 \cosh(p_2 x), \quad (32)$$

where $p_1$ and $p_2$ are the roots of the equation

$$P^4 - L^{II} P^2 + M^{II} = 0, \quad (33)$$

(iii) Region III $(l \le x \le 2l)$ : The solutions of Equations (25) and (26) take the following form:

$$\theta^{*III} = C_1(k_1^2 - p^2)\cosh(k_1 x) + C_2(k_2^2 - p^2)\cosh(k_2 x), \quad (34)$$

$$\sigma^{*III} = a_2 C_1 \cosh(k_1 x) + a_2 C_2 \cosh(k_2 x), \quad (35)$$

## 5. Boundary Conditions

### *5.1. Thermal Boundary Condition*

We suppose that a thermal load is applied to the medium in the two outer sides:

$$\theta(x, y, z, t) = \theta_0 \quad \text{on} \quad x = \pm 2l, \quad (36)$$

### *5.2 Mechanical Boundary Condition*

We consider that the normal stresses disappear on the two sides of the medium. For example,

$$\sigma(x, y, z, t) = 0 \quad \text{on} \quad x = \pm 2l. \quad (37)$$

### *5.3 Continuity Conditions of Heat Flux*

The continuity conditions of heat flux are given as

$$q^I = q^{II} \quad \text{on} \quad x = -l, \quad q^{II} = q^{III} \quad \text{on} \quad x = l, \quad (38)$$

The conditions in Equation (38) can take the following form:

$$\frac{\beta^I}{\left(1 + \tau_q^I \omega + \frac{(\tau_q^2)^I \omega^2}{2}\right)} \frac{\partial \theta^I}{\partial x} = \frac{\beta^{II}}{\left(1 + \tau_q^{II} \omega + \frac{(\tau_q^2)^{II} \omega^2}{2}\right)} \frac{\partial \theta^{II}}{\partial x} \quad \text{on} \quad x = -l,$$

$$\frac{\beta^{II}}{\left(1 + \tau_q^{II} \omega + \frac{(\tau_q^2)^{II} \omega^2}{2}\right)} \frac{\partial \theta^{II}}{\partial x} = \frac{\beta^{III}}{\left(1 + \tau_q^{III} \omega + \frac{(\tau_q^2)^{III} \omega^2}{2}\right)} \frac{\partial \theta^{III}}{\partial x} \quad \text{on} \quad x = l,$$

where the heat flux is subjected to the DPL model of heat conduction. For example,

$$\left(1 + \tau_q \frac{\partial}{\partial t} + \frac{\tau_q^2}{2} \frac{\partial^2}{\partial t^2}\right) q = -K \left(1 + \tau_T \frac{\partial}{\partial t}\right) \frac{\partial \theta}{\partial x}.$$

Employing the normal mode analysis, heat flux takes the following form:

$$q^* = \frac{\beta}{\left(1 + \tau_q \omega + \frac{\tau_q^2 \omega^2}{2}\right)} \frac{\partial \theta^*}{\partial x}.$$

where

$$\beta = -K(1 + \tau_T).$$

### *5.4 Continuity Conditions of Stresses*

The continuity conditions of stresses are given as

$$\sigma^I = \sigma^{II} \quad \text{on} \quad x = -l, \quad \sigma^{II} = \sigma^{III} \quad \text{on} \quad x = l. \quad (39)$$

Applying the above conditions, the stress and temperatures in regions I, II, and III are obtained as follows:

$$\theta^* = \frac{\theta_0^* e^{\omega t} \cos(my + nz)}{(k_1^2 - k_2^2)} \left[ \frac{(k_1^2 - p^2)\cosh(k_1 x)}{\cosh(2lk_1)} - \frac{(k_2^2 - p^2)\cosh(k_2 x)}{\cosh(2lk_2)} \right], \quad -2l \le x \le -l, \; l \le x \le 2l, \quad (40)$$

$$\theta^* = \frac{\theta_0^* e^{\omega t} \cos(my + nz)}{a_2 L(k_1^2 - k_2^2)} \left[ \left\{ \frac{L_{11}}{\cosh(2lk_1)} - \frac{L_{12}}{\cosh(2lk_2)} \right\} \times (p_1^2 - p^2) \cosh(p_1 x) - \left\{ \frac{L_{21}}{\cosh(2lk_1)} - \frac{L_{22}}{\cosh(2lk_2)} \right\} (p_2^2 - p^2)\cosh(p_2 x) \right], \quad -l \le x \le l, \quad (41)$$

$$\sigma^* = \frac{\theta_0^* e^{\omega t}\cos(my+nz)}{(k_1^2-k_2^2)} \left[\frac{\cosh(k_1 x)}{\cosh(2lk_1)} - \frac{\cosh(k_2 x)}{\cosh(2lk_2)}\right], \quad \begin{matrix} -2l \le x \le -l, \\ l \le x \le 2l, \end{matrix} \tag{42}$$

$$\sigma^* = \frac{\theta_0^* e^{\omega t}\cos(my+nz)}{L(k_1^2-k_2^2)} \left[\left\{\frac{L_{11}}{\cosh(2lk_1)} - \frac{L_{12}}{\cosh(2lk_2)}\right\}\cosh(p_1 x) - \left\{\frac{L_{21}}{\cosh(2lk_1)} - \frac{L_{22}}{\cosh(2lk_2)}\right\}\cosh(p_2 x)\right], \quad -l \le x \le l, \tag{43}$$

where

$$L = p_2(p_2^2-p^2)\cosh(p_1 l)\sinh(p_2 l) - p_1(p_1^2-p^2)\sinh(p_1 l)\cosh(p_2 l),$$

$$L_{11} = p_2(p_2^2-p^2)\sinh(p_2 l)\cosh(k_1 l) - a_2\delta_2 k_1(k_1^2-p^2)\cosh(p_2 l)\sinh(k_1 l),$$

$$L_{12} = p_2(p_2^2-p^2)\sinh(p_2 l)\cosh(k_2 l) - a_2\delta_2 k_2(k_2^2-p^2)\cosh(p_2 l)\sinh(k_2 l),$$

$$L_{21} = p_1(p_1^2-p^2)\sinh(p_1 l)\cosh(k_1 l) - a_2\delta_2 k_1(k_1^2-p^2)\sinh(k_1 l)\cosh(p_1 l),$$

$$L_{22} = p_1(p_1^2-p^2)\sinh(p_1 l)\cosh(k_2 l) - a_2\delta_2 k_2(k_2^2-p^2)\sinh(k_2 l)\cosh(p_1 l),$$

where

$$\delta_2 = \frac{\left(1+\tau_q^{II}\omega+\frac{(\tau_q^2)^{II}\omega^2}{2}\right)\beta^I}{\left(1+\tau_q^{I}\omega+\frac{(\tau_q^2)^{I}\omega^2}{2}\right)\beta^{II}} = \frac{\left(1+\tau_q^{II}\omega+\frac{(\tau_q^2)^{II}\omega^2}{2}\right)\beta^{III}}{\left(1+\tau_q^{III}\omega+\frac{(\tau_q^2)^{III}\omega^2}{2}\right)\beta^{II}}.$$

Using Equation (23), we can determine the strain component as follows:

$$e^* = \frac{\theta_0^* e^{\omega t}\cos(my+nz)}{a_2\delta_1(k_1^2-k_2^2)} \left[\frac{(k_1^2-p^2+a_2)\cosh(k_1 x)}{\cosh(2lk_1)} - \frac{(k_2^2-p^2+a_2)\cosh(k_2 x)}{\cosh(2lk_2)}\right], \quad \begin{matrix} -2l \le x \le -l, \\ l \le x \le 2l, \end{matrix} \tag{44}$$

$$e^* = \frac{\theta_0^* e^{\omega t}\cos(my+nz)}{a_2\delta_1 L(k_1^2-k_2^2)} \left[\left\{\frac{L_{11}}{\cosh(2lk_1)} - \frac{L_{12}}{\cosh(2lk_2)}\right\} \times(p_1^2-p^2+a_2)\cosh(p_1 x) - \left\{\frac{L_{21}}{\cosh(2lk_1)} - \frac{L_{22}}{\cosh(2lk_2)}\right\} (p_2^2-p^2+a_2)\cosh(p_2 x)\right], \quad -l \le x \le l, \tag{45}$$

Furthermore, using Equation (18), we can determine the displacement component as follows:

$$u^* = R_4\sinh(\lambda_u x) + \frac{l_1}{k_1^2-\lambda_u^2}\sinh(k_1 x) - \frac{l_2}{k_2^2-\lambda_u^2}\sinh(k_2 x), \quad \begin{cases} -2l \le x \le -l, \\ l \le x \le 2l, \end{cases} \tag{46}$$

$$u^* = R_5\cosh(\lambda_u x) + \frac{l_3}{p_1^2-\lambda_u^2}\sinh(p_1 x) - \frac{l_4}{p_2^2-\lambda_u^2}\sinh(p_2 x), \quad -l \le x \le l, \tag{47}$$

where

$$l_1 = \frac{\theta_0^* e^{\omega t}\cos(my+nz)}{a_2\delta_2\delta_1(k_1^2-k_2^2)\cosh(2lk_1)} \times\left\{k_1(k_1^2-p^2)(\delta_1+\delta_2-1) - a_2 k_1(1-\delta_2)\right\},$$

$$l_2 = \frac{\theta_0^* e^{\omega t}\cos(my+nz)}{a_2\delta_2\delta_1(k_1^2-k_2^2)\cosh(2lk_2)} \times\left\{k_2(k_2^2-p^2)(\delta_1+\delta_2-1) - a_2 k_2(1-\delta_2)\right\},$$

$$l_3 = \frac{\theta_0^* e^{\omega t}\cos(my+nz)}{a_2 L\delta_1(k_1^2-k_2^2)} \left\{\frac{L_{11}}{\cosh(2lk_1)} - \frac{L_{12}}{\cosh(2lk_2)}\right\} \times\left\{p_1(p_1^2-p^2)(\delta_1+\delta_2-1) - p_1 a_2(1-\delta_2)\right\},$$

$$l_4 = \frac{\theta_0^* e^{\omega t}\cos(my+nz)}{a_2 L\delta_1(k_1^2-k_2^2)} \left\{\frac{L_{21}}{\cosh(2lk_1)} - \frac{L_{22}}{\cosh(2lk_2)}\right\} \times\left\{p_2(p_2^2-p^2)(\delta_1+\delta_2-1) - p_2 a_2(1-\delta_2)\right\},$$

$$R_4 = \frac{1}{\lambda_u\cosh(2l\lambda_u)} \left[\frac{\delta_1+2\delta_2-1}{2\delta_2\delta_1}\theta_0^{\blacklozenge} + \frac{l_2 k_2}{k_2^2-\lambda_u^2}\cosh(2lk_2) - \frac{l_1 k_1}{k_1^2-\lambda_u^2}\cosh(2lk_1)\right],$$

$$R_5 = \frac{1}{\lambda_u \cosh(2l\lambda_u)}\left[\frac{\delta_1 + 2\delta_2 - 1}{2\delta_2\delta_1}\theta_0^{\blacklozenge} + \frac{l_4 p_2}{p_2^2 - \lambda_u^2}\cosh(2lp_2) - \frac{l_3 p_1}{p_1^2 - \lambda_u^2}\cosh(2lp_1)\right],$$

where

$$\lambda_u^2 = m^2 + n^2 + \frac{\omega^2}{\delta}.$$

## 6. Numerical Results and Discussions

The aim of this section is to illustrate the results obtained in the preceding sections. First, we present the analytical numerical results. For the numerical computations, we have considered a copper-like material for layers I and III, and stainless steel for layer II. Since $\omega$ is the complex time constant, we have $\omega = \omega_0 + i\zeta$ then $e^{\omega t} = e^{\omega_0 t}(\cos\zeta t + i\sin\zeta t)$. The values of the material constants for the copper (layers I and III) are

$\alpha_T = 17.8\times10^{-6}$ K$^{-1}$, $\rho = 8954$ kg.m$^{-3}$, $c_E = 383.1$ m$^2$.K$^{-1}$m$^{-2}$,
$K = 386$ kg.m.K$^{-1}$.m$^{-3}$, $T_0 = 293$ K, $\mu/\lambda = 0.497425$,
$\varepsilon = 0.0150$, $\tau_T = 0.01$, $\tau_q = 0.2$

The values of the material constants for stainless steel (layer II) are

$\alpha_T = 17.7\times10^{-6}$ K$^{-1}$, $\rho = 7970$ kg.m$^{-3}$, $c_E = 561$ m$^2$.K$^{-1}$m$^{-2}$,
$K = 195$ kg.m.K$^{-1}$.m$^{-3}$, $T_0 = 293$ K, $\mu/\lambda = 0.700680$,
$\varepsilon = 0.0141$, $\tau_T = 0.01$, $\tau_q = 0.2$

Furthermore, the values of the other non-dimensional parameters are $\theta_0^* = 1$, $m = 1.2$, $n = 1.3$, $\omega_0 = 1.0$, $\zeta = 0.2$. Figures 1–4 have been plotted to study the variation of the temperature, stress, strain, and displacement against the distance $x$ for the DPL model at $t = 0.1$ s and 0.4 s when the depths of the layer are at $y = z = 0.1$ and $y = z = 0.5$, respectively. In the figures, the continuous lines correspond to $y = z = 0.1$, while the dotted lines correspond to $y = z = 0.5$.

Figure 2 depicts the variation of the temperature $\theta$ versus distance $x$ for different depths at $t = 0.1$ and $0.4$. As the temperature attains its maximum magnitude on the two outer sides of the sandwich structure to satisfy the thermal boundary conditions of the problem, the magnitude of $\theta$ decreases sharply toward layer II of the sandwich structure at $y = z = 0.1$. In addition, the magnitude of $\theta$ for regions I and III (copper) is greater than the magnitude of $\theta$ in region II (stainless steel). Furthermore, at depth $y = z = 0.5$, the magnitude of $\theta$ decreases slowly compared with the rate at $y = z = 0.1$. As time $t$ increases, the magnitude of the temperature also increases; however, as the depth of the composite medium increases, the magnitude of $\theta$ decreases.

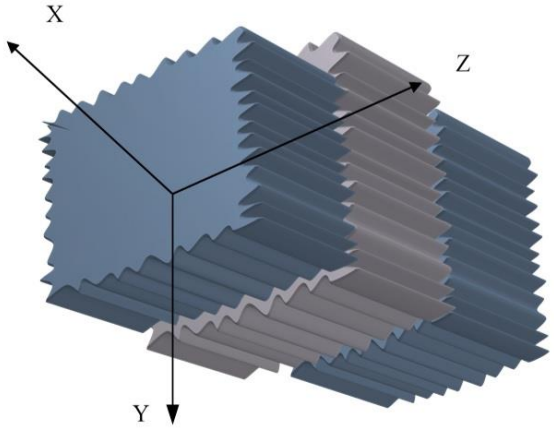


**Figure 1.** Geometry of the Problem

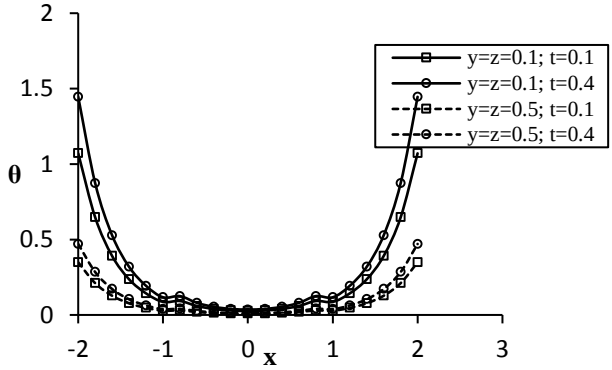


**Figure 2.** Variation of temperature $\theta$ against $x$ for the DPL model at $t = 0.1$ and $0.4$

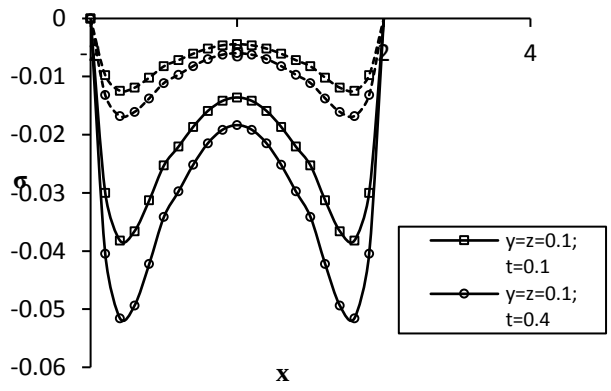


**Figure 3.** Variation of stress $\sigma$ against $x$ for the DPL model at $t = 0.1$ and $0.4$

Fig. 3 shows the variation of the stress $\sigma$ against the distance $x$ at $t = 0.1$ and 0.4 and for different depths of the sandwich structure ( $y = z = 0.1$ and $y = z = 0.5$, respectively). The stress $\sigma$ has a value of zero on both outer sides of the sandwich structure, which satisfies the mechanical boundary condition of the problem given in Equation (37). Furthermore, the stress $\sigma$ is compressive in nature near the two planes of application of thermal loading for different depths of the medium. For different $y$ and $z$, the magnitude of $\sigma$ for stainless steel is less than the $\sigma$ of the copper. As the depth of the layer increases, the magnitude of $\sigma$ decreases throughout the body. In addition, an increase in time also increases the magnitude of $\sigma$.

Fig. 4 shows the variation of the strain $e$ against distance $x$ for different values of depth at $t = 0.1$ and 0.4. The magnitude of $e$ is greater for copper than for stainless steel. In addition, the strain is maximum near the two outer boundaries of the sandwich structure. The magnitude decreases sharply as we move toward layer II. With an increase in depth, the magnitude of elongation decreases.

Fig. 5 shows the variation of displacement $u$ against the distance $x$ for $t = 0.1$ and 0.4. The magnitude of the displacement increases at intervals $-2 < x < -1.9$ and $1.9 < x < 2$ to attain the maximum magnitude near $x = \pm 1.9$. The magnitude then decreases sharply as we move toward layer II when $y = z = 0.1$. Furthermore, the displacement magnitude almost negligible near the two outer surfaces of the sandwich structure at the interval $-0.5 < x < 0.5$.

The figures show that $x = \pm l$ at the interfaces of the composite structure because the medium satisfies the continuity conditions of heat flux and stress as given in Equations (38) and (39), respectively. Thus, the graphical representations of the thermophysical quantities are compatible with the continuity conditions at the interfaces.

Figs. 6–9 have been plotted to study the profile of variation of the thermophysical quantities for $-2 < x < 2$ and $t = 0.1 \ldots 0.5$ at depth $y = z = 0.1$. The figures show that as time increases, the profile of the thermophysical quantities also increase, which is quite plausible.

Figs. 10–13 show the variation of the thermophysical quantities for the same set of parameters as mentioned earlier at $y = z = 0.2$. The figures show that as the depth increases, the magnitudes of the thermophysical quantities decrease. However, as time increases, the magnitudes increase.

Figs. 14 and 15 show the variation of the stress $(\sigma)$ and displacement $(u)$, respectively, against the thickness of the sandwich structure at depth $y = z = 0.1$ and time $t = 0.1$ and 0.4 for both the LS and the DPL models.

Fig. 14 shows that for both the LS and the DPL models, the $\sigma$ value become zero on the two outer sides of the sandwich structure, which satisfies the mechanical boundary condition of the problem. Furthermore, for $t = 0.1$ and 0.4, the magnitude of $\sigma$ for the LS model is greater than in the DPL model.

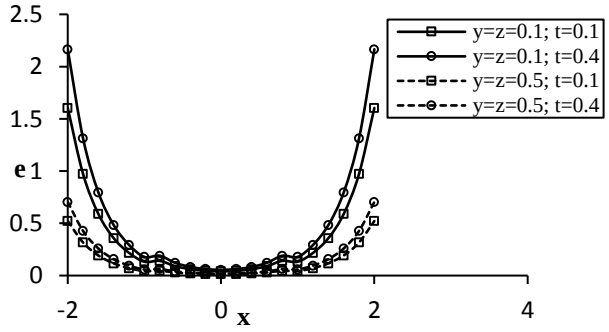


**Fig. 4.** Variation of strain $e$ against $x$ for the DPL model at $t = 0.1$ and 0.4

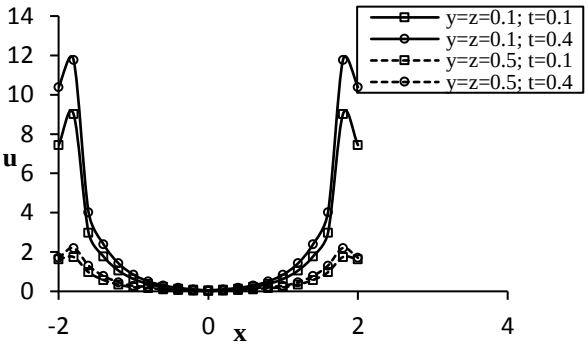


**Figure 5.** Variation of displacement $u$ against $x$ for the DPL model when $t = 0.1$ and 0.4

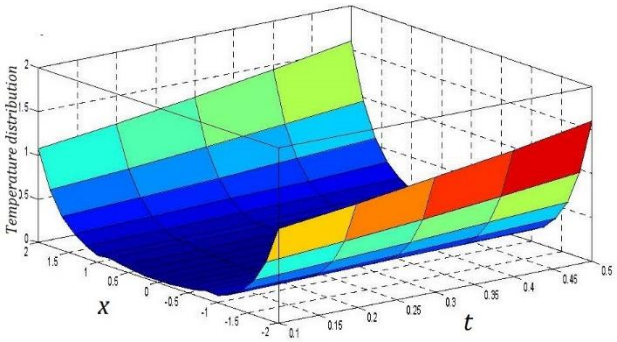


**Figure 6.** Profile of temperature $\theta$ for the DPL model for different $x$ and $t$ at $y = z = 0.1$

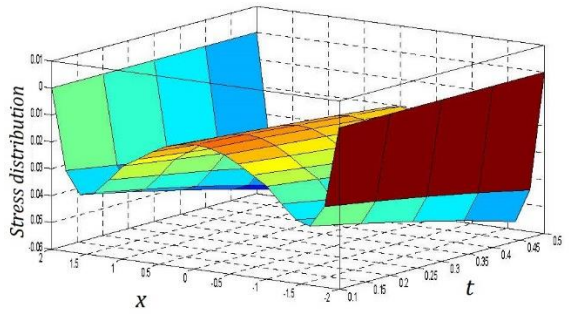


**Figure 7.** Profile of stress $\sigma$ for the DPL model for different $x$ and $t$ at $y = z = 0.1$

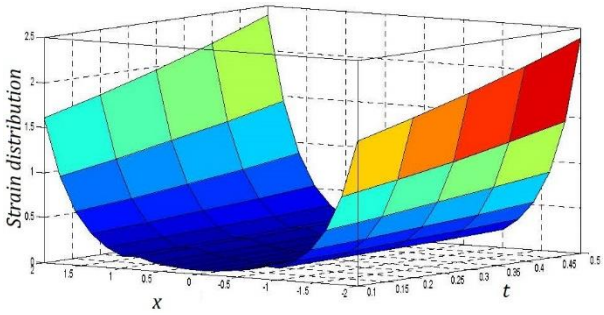


**Figure 8.** Profile of strain $e$ for the DPL model for different $x$ and $t$ when $y = z = 0.1$

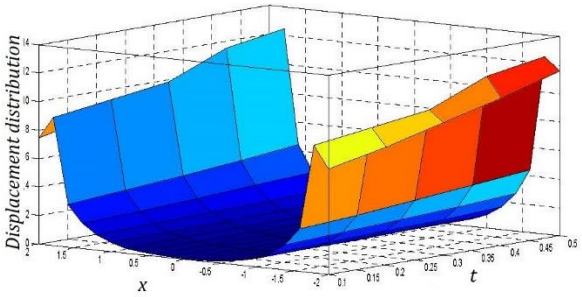


**Figure 9.** Profile of displacement $u$ for the DPL model for different $x$ and $t$ at $y = z = 0.1$

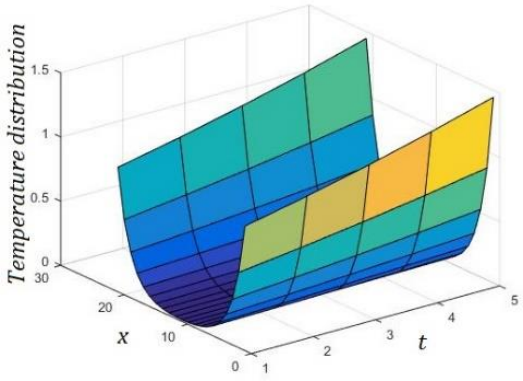


**Figure 10.** Profile of temperature $\theta$ for the DPL model for different $x$ and $t$ at $y = z = 0.2$

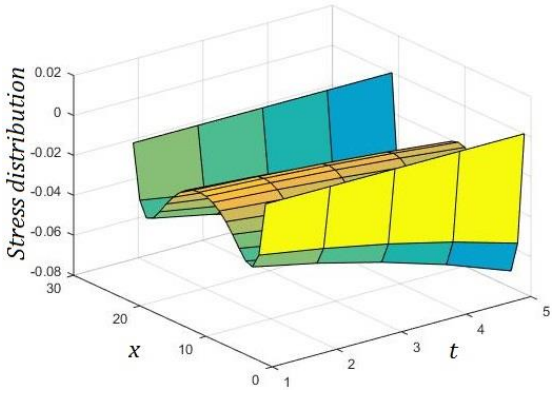


**Figure 11.** Profile of stress $\sigma$ for the DPL model for different $x$ and $t$ at $y = z = 0.2$

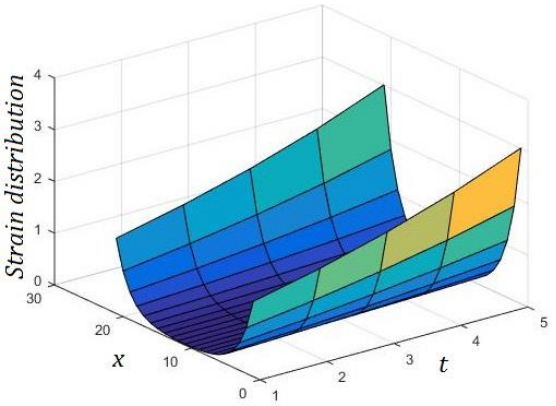


**Figure 12.** Profile of strain $e$ for the DPL model for different $x$ and $t$ at $y = z = 0.2$

Fig. 15 shows the variation of the displacement $u$ for the same set of parameters as mentioned earlier. The magnitude of $u$ for the LS model is greater than in the DPL model for both earlier situations and later on.

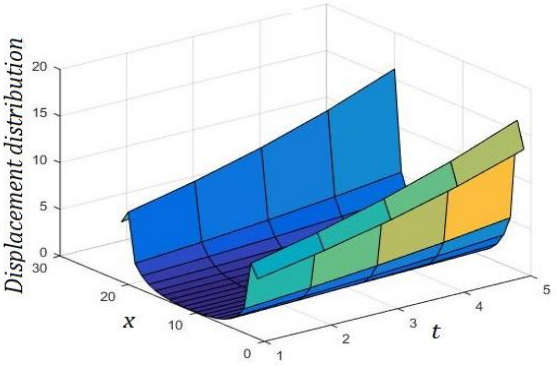


**Figure 13.** Profile of displacement $u$ for the DPL model for different $x$ and $t$ at $y = z = 0.2$ .

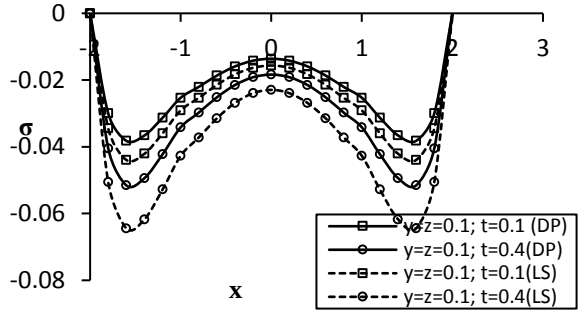


**Figure 14.** Variation of stress $\sigma$ against $x$ for the DPL and LS models at $t = 0.1$ and $0.4$

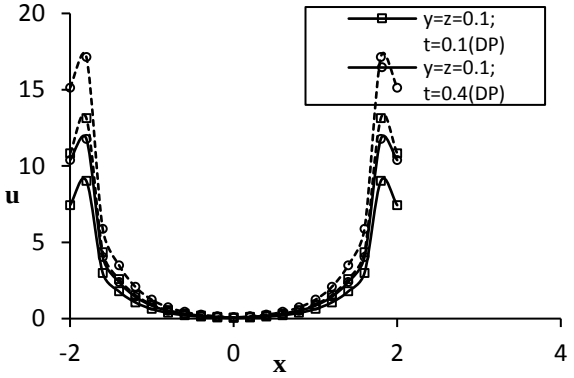


**Figure 15.** Variation of displacement $u$ against $x$ for the DPL and LS models at $t = 0.1$ and $0.4$

Fig. 16 shows the variation of the stress component $\sigma_{xx}$ against the distance $x$ for the DPL model for $y = z = 0.5$ and $y = z = 0.1$. The temperature on both sides of the structure is considered to be constant. The stresses have a significant effect on the structure as observed in Fig. 11. The magnitude of the stress component is the same on both boundaries of the structure. The magnitude of the profile of the stress component increases as we move within the medium.

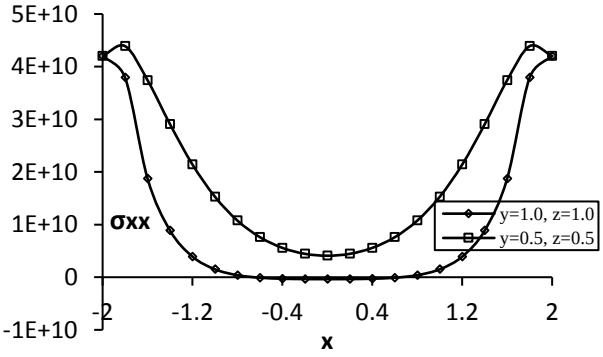


**Figure 16.** Variation of stress $\sigma_{xx}$ against $x$ for the DPL and LS models at $t = 0.4$

## 7. Conclusions

In this paper, a mathematical treatment has been presented to explore the wave propagation in a three-dimensional isotropic thermoelastic medium based on the DLP model. The LS model can be obtained as a particular case. The problem has been solved theoretically and exemplified through the use of the LS and DPL models. All the figures exhibit the different peculiarities that occur during the propagation of waves. The conclusions may be summarized as follows.

1. Significant differences in the variation of the thermophysical quantities for the LS and DPL models can be observed. In the case of generalized thermoelasticity, for a high heat flux over a very short time, the heat conduction calculation based on the DPL model is more advantageous than the LS model in engineering problems.
2. The DPL thermoelastic model has significant advantages compared with the single phase lag thermoelastic model where $\tau_T$ is the phase lag of the temperature gradient. In the DPL model with $\tau_q > \tau_T$, the temperature gradient within the medium induces heat flux; hence, the temperature gradient is the cause of the energy transport and the heat flux is the effect. However, for $\tau_q < \tau_T$, heat flux is the cause of the energy transport and the temperature gradient is the effect. For $\tau_q = \tau_T$ with a homogeneous initial temperature, the DPL model reduces to Fourier's law. While heat flux appears for a very small time interval in an elastic body, it is more advantageous to consider the DPL model rather than the LS model because the stability in the variation of the thermophysical quantities are more prominent in the DPL model.
3. The magnitude of the thermophysical quantities are greater for copper (layers I and III) than for stainless steel (layer II).
4. The magnitudes of the thermophysical quantities increase with the increase of time $t$.
5. The magnitudes of the thermophysical quantities are greater for the LS model than the DPL model for both the earlier situation and later on.
6. The present work can be considered as a of generalized thermoelasticity problem in the context of the DPL thermoelastic model. It can also be considered to be an application of a problem that occurs in several engineering fields in which a high heat flux appears in an elastic body for a very short time interval.

## Acknowledgements

We are grateful to Prof. S. C. Bose of the Department of Applied Mathematics, University of Calcutta for his valuable suggestions and guidance in preparation of this paper. We also express our sincere thanks to the reviewers for their valuable suggestions on ways to improve the paper.

## References

[1] Lord H, Shulman Y, A generalized dynamical theory of thermoelasticity. *Jounal of Mechanics and Physics of Solids* 1967; 15:299-309.

[2] Green AE, Lindsay KA, Thermoelasticity. *Journal of Elasticity* 1972:2:1-7.

[3] Green AE, Naghdi PM, A re-examination of the basic results of thermomechanics. *Proceedings of Royal Society London, Series A* 1991:432: 171-194.

[4] Green AE, Nagdhi PM, Onundamped heat waves in an elastic solid. *Journal of Thermal Stresses* 1992:15:252-264.

[5] Green AE, Nagdhi PM, Thermoelasticity without energy dissipation. *Journal of Elasticity* 1993:31:189-208.

[6] Tzou DY, Ozisik MN, Chieffelle R J, The lattice temperature in the microscopic two-step model, *ASME Journal of heat transfer* 1994:116: 1034-1038.

[7] Tzou DY, A unified field approach for heat conduction from macro to micro scales. *ASME Journal of Heat Transfer* 1995:117:8-16.

[8] Chandrasekharaiah DS, Hyperbolic thermoelasticity: A review of recent literature. *Applied Mechanics Review* 1998:51:705-729.

[9] Tzou DY, Macro to Micro-scale Heat transfer: The lagging behavior, *Taylor and Francis, New York*, 1997:1-64.

[10] Prasad R, Kumar R Mukhopadhyay S, Propagation of harmonic plane waves under thermoelasticity with dual-phase-lags. *International Journal of Engineering Science* 2010:48:2028-2043.

[11] El-Karamany AS, Ezzat MA, On the dual-phase-lag thermoelasticity theory. *Meccanica* 2014:49:79-89.

[12] Chiriţă S. On the time differential dual-phase-lag thermoelastic model. *Meccanica* 2016: DOI: 10.1007/s11012-016-0414-2.

[13] Sur A, Kanoria M, Fractional heat conduction with finite wave speed in a thermo-visco-elastic spherical shell. *Latin American Journal of Solids and Structures* 2014:11(7):1132-1162.

[14] Sur A, Kanoria M. Modeling of memory-dependent derivative in a fibre-reinforced plate. *Thin-Walled Structures*. 2018; 126:85-93.

[15] Sur A, Pal P, Kanoria M. Modeling of memory-dependent derivative in a fiber-reinforced plate under gravitational effect. *Journal of Thermal Stresses* 2018; 41(8):973-92.

[16] Sur A, Kanoria M. Propagation of thermal waves in a functionally graded thick plate. *Mathematics and Mechanics of Solids* 2017; 22(4):718-36.

[17] Youssef HM, El-Bary AA. Thermal shock problem of a generalized thermoelastic layered composite material with variable thermal conductivity. *Mathematical Problems in Engineering* 2006; 2006.

[18] Zenkour AM, Mashat DS, Abouelregal AE. The effect of dual-phase-lag model on reflection of thermoelastic waves in a solid half space with variable material properties. *Acta Mechanica Solida Sinica* 2013:26(6):659-670.

[19] Abbas IA, Zenkour AM, Dual-Phase-Lag Model on Thermoelastic Interactions in a Semi-Infinite Medium Subjected to a Ramp-Type Heating. *Journal of Computational and Theoretical nanosciences* 2014:11(3): 642-645.

[20] Zenkour AM, Abouelregal AE, Effects of phase-lags in a thermoviscoelastic orthotropic continuum with a cylindrical hole and variable thermal conductivity. *Archives of Mechanics* 2015: 67(6): 457-475.

[21] Zenkour AM, Two-Dimensional Coupled Solution for Thermoelastic Beams via Generalized Dual-Phase-Lags Model. *Mathematical Modelling and analysis* 2016: 21(3): 319-335.

[22] Zenkour AM, A generalized thermoelastic dual-phase-lagging response of thick beams subjected to harmonically varying heat and pressure. *Journal of Theoretical and Applied Mechanics* 2018: 53(1): 15-30.

[23] Guz AN, Elastic Waves in a Body with Initial Stresses I. General Theory, *NaukovaDumka, Kiev (in Russian)* 1986.

[24] Guz AN, Elastic Waves in a Body with Initial Stresses II. Propagation Laws, *NaukovaDumka, Kiev, (in Russian)* 1986.

[25] Guz AN, Elastic Waves in Bodies with Initial (Residual) Stresses, *A.S.K., Kiev, (in Russian*) 2004.

[26] Vishwakarma SK, Torsional wave propagation in a self-reinforced medium sandwiched between a rigid layer and a viscoelastic half-space under gravity. *Applied Mathematics and Computation* 2014:242:1-9.

[27] Tokovyy Y, Ma CC, Analytical solutions to the axisymmetric elasticity and thermoelasticity problems for a arbitrary inhomogeneous layer.

*International Journal of Engineering Science* 2015:92:1-7.

[28] Wu GC, The analytic theory of the temperature fields of bituminous pavement over semi-rigid road base. *Applied Mathematics and Mechanics* 1997:18:181-190.

[29] Ootao Y, Tanigawa Y, Transient analysis of multilayered magneto-electro-thermoelastic strip due to nonuniform heat supply. *Composte Structures* 2005:68:471-480.

[30] Zhong Y, Geng LT, Thermal stresses of asphalt pavement under dependence of material characteristics on reference temperature. *Mechanics of Time Dependent Materials* 2009:3: 81-91

[31] Sur A, Kanoria M, Fibre reinforced magneto thermoelastic rotating medium with fractional heat conduction. Procedia Engineering 2015:127:605-612.